

## ON THE IMPEDANCE OF GALVANIC CELLS

### XXVI. APPLICATION OF THE COMPLEX PLANE METHOD IN THE CASE OF MIXED CURRENTS

B. G. DEKKER, M. SLUYTERS-REHBACH AND J. H. SLUYTERS

*Laboratory of Analytical Chemistry, State University, Utrecht (The Netherlands)*

(Received March 22nd, 1969)

#### INTRODUCTION

The impedance of a galvanic cell has proved to be a very useful datum for the study of faradaic processes and double-layer phenomena at the electrode-solution interface<sup>1,2</sup>. In general, the kinetic parameters and the double-layer capacity can be obtained by analysis of the impedance data according to the complex plane method<sup>2</sup>. Procedures for analysing data have been proposed for a number of cases, limited, however, to electrode processes with one electrode reaction proceeding.

Within the framework of our study on the hydrogen evolution on mercury in concentrated acid solutions<sup>3</sup>, the impedance of the mercury electrode in a concentrated HI solution was measured. It was found that this system gives rise to the appearance of a so-called mixed current caused by the simultaneous occurrence of two electrode reactions, *viz.* the Hg/HgI<sub>4</sub><sup>2-</sup> reaction and the H<sup>+</sup>/H<sub>2</sub>(Hg) reaction.

The aim of this paper is to investigate the applicability of the complex plane method to cases of mixed currents.

#### ANALYSIS OF CELL IMPEDANCES IN THE CASE OF TWO SIMULTANEOUSLY PROCEEDING ELECTRODE REACTIONS

We confine our discussion to the simultaneous proceeding of two electrode reactions because the equations for more than two processes are somewhat cumbersome. Moreover, it will appear that the results in that case are trivial or that the complex plane method is not feasible.

Two simple electrode reactions are considered, *i.e.* the exchange of  $n_i$  electrons occurs in one charge transfer step, in the absence of coupled chemical reactions and of chemical reactions between the components in the solution.



Both reactions will be characterized by a large number of factors, such as the electrode potential,  $E$ , the standard potentials,  $E^\circ$ , the specific heterogeneous rate constants,  $k_{sh}$ , the transfer coefficients,  $\alpha$ , the diffusion coefficients,  $D$ , the temperature, and the initial presence of Ox and Red. The complex plane analysis yields the values of the impedance parameters  $\theta_i$  (transfer resistances) and  $\sigma_i$  (Warburg coefficients) and  $C_d$  (double-layer capacity), eventually as a function of  $E$ . Once these are known, an

attempt can be made to calculate the values of  $k_{sh}$ ,  $\alpha$  and  $D$  from the parameters obtained using the equations derived by Timmer *et al.*<sup>4</sup>

It is known from d.c. polarography that in the case of several simultaneously proceeding oxidation or reduction reactions, the d.c. current at a certain potential is equal to the algebraic sum of the currents for each process. Wagner and Traud<sup>5</sup> showed that the same additivity holds for the superposition of an anodic and a cathodic wave. It is reasonable to assume that this also holds for a.c. currents, which means that two faradaic impedances  $Z_{F_1}$  and  $Z_{F_2}$  in parallel appear in the equivalent circuit of the cell impedance, given by<sup>1</sup>

$$Z_{F_i} = \theta_i + \sigma_i \omega^{-\frac{1}{2}}(1-j) \quad (3)$$

where  $\omega$  is the angular a.c. frequency and  $j = \sqrt{-1}$ , the imaginary unit. The equivalent circuit of the cell impedance is presented in Fig. 1, where  $R_\Omega$  is the ohmic resistance of the cell and  $C_d$  the double-layer capacity. Note that in this modified Randles circuit<sup>1</sup>, possible (strong) specific adsorption of reactants has not been considered<sup>6</sup>.

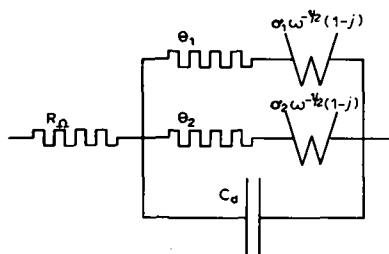


Fig. 1. Equivalent circuit of the impedance of a galvanic cell with two simultaneously proceeding electrode reactions.

The usual procedure in the analysis is the calculation of the real and imaginary components of the admittance of the electrode-solution interface (electrode admittance) after subtraction of  $R_\Omega$  from the real part of the cell impedance,  $Z'$ , and combination of the remainder with the imaginary part,  $Z''$ :

$$Y'_{el} = \frac{Z' - R_\Omega}{(Z' - R_\Omega)^2 + (Z'')^2} \quad (4a)$$

$$Y''_{el} = \frac{Z''}{(Z' - R_\Omega)^2 + (Z'')^2} \quad (4b)$$

It follows from Fig. 1 and eqn. (3) that

$$Y'_{el} = \frac{1}{\sigma_1 \omega^{-\frac{1}{2}}} \frac{p_1 + 1}{p_1^2 + 2p_1 + 2} + \frac{1}{\sigma_2 \omega^{-\frac{1}{2}}} \frac{p_2 + 1}{p_2^2 + 2p_2 + 2} \quad (5a)$$

$$Y''_{el} = \frac{1}{\sigma_1 \omega^{-\frac{1}{2}}} \frac{1}{p_1^2 + 2p_1 + 2} + \frac{1}{\sigma_2 \omega^{-\frac{1}{2}}} \frac{1}{p_2^2 + 2p_2 + 2} + \omega C_d \quad (5b)$$

where the irreversibility quotients,  $p_i$ , are defined by

$$p_i = p'_i \omega^{\frac{1}{2}} = \frac{\theta_i}{\sigma_i \omega^{-\frac{1}{2}}} \quad (6)$$

These equations are generally valid for reversible as well as irreversible reactions.

It can be seen that the value of  $C_d$  need not be known for the evaluation of  $\theta_i$  and  $\sigma_i$  (eqn. (5a)) which is an outstanding feature of the complex plane method. As a particular advantage of the method,  $C_d$  can be determined in the presence of the electrode reactions if  $\theta_i$  and  $\sigma_i$  are known (see eqn. (5b)). This is especially important for those cases where  $C_d$  cannot be measured in the absence of electroactive species<sup>7</sup>. In this paper  $C_d$  will be considered as unknown.

#### Evaluation of $\theta_i$ , $\sigma_i$ and $C_d$

The frequency-dependence of  $Y'_{ei}$  at a fixed potential is, in the complex plane analysis, the criterion of the extent to which an electrode reaction is reversible. The reaction behaves reversibly if  $Y'_{ei}$  increases linearly with  $\omega^{\frac{1}{2}}$  within the range covered by the measurements, normally between  $\omega_1 = 2 \times 10^3$  and  $\omega_2 = 2 \times 10^4 \text{ s}^{-1}$ . The reaction may be said to be irreversible if  $Y'_{ei}$  is independent of  $\omega^{\frac{1}{2}}$  in the frequency range mentioned. In the case of one electrode reaction, the values of  $p'$ ,  $\sigma$  and  $\theta$  can be evaluated from the frequency-dependence of  $Y'_{ei}$  by a curve-fitting procedure, cf. ref. 8. In the following it will be discussed for which values of  $p'_1$  and  $p'_2$  the values of  $\theta_1$ ,  $\theta_2$ ,  $\sigma_1$  and  $\sigma_2$  can be determined from the frequency-dependence of the total electrode admittance.

When it is assumed that neither of the electrode reactions has a negligible contribution to the total electrode admittance, it is useful to consider three cases: (A)  $p'_1 \approx p'_2$ , (B)  $p'_1 \neq p'_2$  where  $3 \times 10^{-3} < p'_i < 3 \times 10^{-1}$  and (C)  $p'_1 \ll p'_2$ .

#### (A) $p'_1 \approx p'_2$

##### (i) $3 \times 10^{-3} < p'_i < 3 \times 10^{-1}$

In Fig. 2 values of  $Y'_{ei}$  for reaction 1 (curve 1) and 2 (curve 2) and of the sum-admittance (curve 3) are represented as a function of  $\omega^{\frac{1}{2}}$ ; the values are calculated numerically, using the data:  $\theta_1 = 6 \text{ } \Omega \text{ cm}^2$ ,  $\sigma_1 = 200 \text{ } \Omega \text{ cm}^2 \text{ s}^{-\frac{1}{2}}$ ,  $\theta_2 = 15 \text{ } \Omega \text{ cm}^2$  and  $\sigma_2 = 500 \text{ } \Omega \text{ cm}^2 \text{ s}^{-\frac{1}{2}}$  (i.e.  $p'_1 = p'_2 = 3 \times 10^{-2}$ ). From Fig. 2 it appears that  $Y'_{ei}$  increases non-linearly in the above-mentioned frequency range for all three curves. This means that curve (3) is composed of the admittances of two quasi-reversible electrode reactions. From the frequency-dependence of  $Y'_{ei}$  the value of  $p'_1$  ( $= p'_2$ ) can be deter-

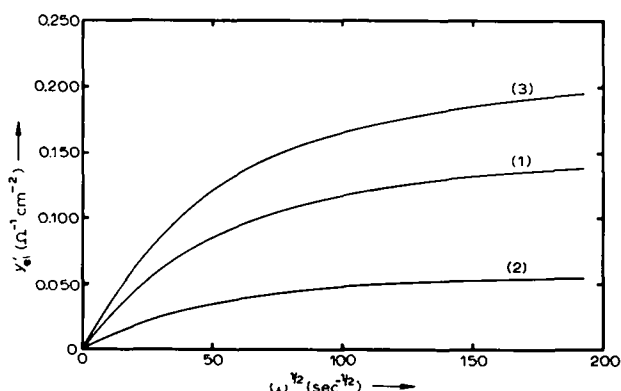


Fig. 2. Plots of  $Y'_{ei}$  vs.  $\omega^{\frac{1}{2}}$ : (1)  $p'_1 = 3 \times 10^{-2}$ ,  $\theta_1 = 6 \text{ } \Omega \text{ cm}^2$ ,  $\sigma_1 = 200 \text{ } \Omega \text{ cm}^2 \text{ s}^{-\frac{1}{2}}$ ; (2)  $p'_2 = 3 \times 10^{-2}$ ,  $\theta_2 = 15 \text{ } \Omega \text{ cm}^2$ ,  $\sigma_2 = 500 \text{ } \Omega \text{ cm}^2 \text{ s}^{-\frac{1}{2}}$ ; (3) sum of (1) and (2).

mined in the usual way, *i.e.* by a curve-fitting procedure using eqn. (5a). However, it is not possible to evaluate the separate values of  $\theta_1$ ,  $\sigma_1$ ,  $\theta_2$  and  $\sigma_2$ . In this case the substitution values are found:

$$\theta_s = \frac{\theta_1 \theta_2}{\theta_1 + \theta_2} \quad \text{and} \quad \sigma_s = \frac{\sigma_1 \sigma_2}{\sigma_1 + \sigma_2}$$

Insertion of the results into eqn. (5b) gives  $C_d$ .

$$(ii) p'_1 < 3 \times 10^{-3}$$

In this case both reactions behave reversibly in the frequency range mentioned. From the slope of the  $Y'_{el}$  (sum) vs.  $\omega^{\frac{1}{2}}$  plot (which is a straight line with zero intercept) the value of  $\sigma_s$  can be calculated. It can be derived from eqns. (5) that  $C_d$  can be calculated from

$$C_d = \frac{Y''_{el} - Y'_{el}}{\omega} \quad (7)$$

$$(iii) p'_1 > 3 \times 10^{-1}$$

In this case both reactions behave irreversibly in the frequency range mentioned.  $Y'_{el}$  (sum) is independent of frequency and equals  $1/\theta_s$ . The value of  $C_d$  can be obtained from eqn. (5b) which becomes:

$$Y''_{el} = \omega C_d \quad (8)$$

Thus, in the particular case where  $p'_1 = p'_2$ , the sum-admittance behaves as if one electrode reaction is proceeding. When  $p'_1$  is almost equal to  $p'_2$ , the same results will be obtained with a relatively small error. If the measurements could be performed at much higher frequencies (*e.g.* in case (i)  $\omega^{\frac{1}{2}} \gg 200 \text{ s}^{-\frac{1}{2}}$ ) both reactions behave irreversibly, and at measurements at very low frequencies (*e.g.* in case (i)  $\omega^{\frac{1}{2}} < 10 \text{ s}^{-\frac{1}{2}}$ ) both reactions behave reversibly. For these cases the same results would be obtained as have already been discussed above.

$$(B) p'_1 \neq p'_2 \text{ where } 3 \times 10^{-3} < p'_1 < 3 \times 10^{-1}$$

It appears from eqns. (5) that the impedance parameters,  $\theta_i$  and  $\sigma_i$ , and hence the values of  $C_d$ , can be evaluated from the frequency dispersion of the sum-admittance by applying a mathematical variation procedure. However, in general this will not be feasible in view of the accuracy of the  $Y'_{el}$  values, the limited frequency region of the measurements, and the large number of parameters.

If the measurements could be performed at very high (*e.g.*  $\omega^{\frac{1}{2}} \gg 200 \text{ s}^{-\frac{1}{2}}$ ) or very low (*e.g.*  $\omega^{\frac{1}{2}} \ll 10 \text{ s}^{-\frac{1}{2}}$ ) frequencies the values of  $\theta_s$  and  $\sigma_s$  could be obtained, and hence also the values of  $C_d$  for both cases.

$$(C) p'_1 \ll p'_2$$

(i) In Fig. 3, numerically calculated values of  $Y'_{el}$  for reaction 1 (curve 1) and 2 (curve 2) and values of the sum-admittance (curve 3) are represented as a function of  $\omega^{\frac{1}{2}}$ ; the data used for the calculation are:  $\theta_1 = 1.5 \text{ } \Omega\text{cm}^2$ ,  $\sigma_1 = 500 \text{ } \Omega\text{cm}^2\text{s}^{-\frac{1}{2}}$  (*i.e.*  $p'_1 = 3 \times 10^{-3}$ ) and  $\theta_2 = 30 \text{ } \Omega\text{cm}^2$ ,  $\sigma_2 = 100 \text{ } \Omega\text{cm}^2\text{s}^{-\frac{1}{2}}$  (*i.e.*  $p'_2 = 3 \times 10^{-1}$ ).

It can be seen in Fig. 3 that in the frequency range normally covered by the measurements, the sum-admittance (curve 3) is composed of the admittances of a reversible (curve 1) and an irreversible electrode reaction (curve 2). In this case, eqn. (5a) reduces to:

$$Y'_{el} = \frac{\omega^{\frac{1}{2}}}{2\sigma_1} + \frac{1}{\theta_2} \quad (9a)$$

The  $Y'_{el}$  vs.  $\omega^{\frac{1}{2}}$  plot is a straight line as in case (Aii) but now it has an intercept  $1/\theta_2$ . From the slope and the intercept of the plot the values of both  $\sigma_1$  and  $\theta_2$  are readily obtained. Since eqn. (5b) reduces to

$$Y''_{el} = \frac{\omega^{\frac{1}{2}}}{2\sigma_1} + \omega C_d \quad (9b)$$

the values of  $C_d$  can be calculated by insertion into this equation of the  $\sigma_1$  values found.

Figure 3 illustrates once more that both the values of  $p'_i$  and the frequency range in which the measurements are performed are important for the possibility of evaluating the impedance parameters from the  $Y'_{el}$  vs.  $\omega^{\frac{1}{2}}$  plot. Two other combinations have to be considered:

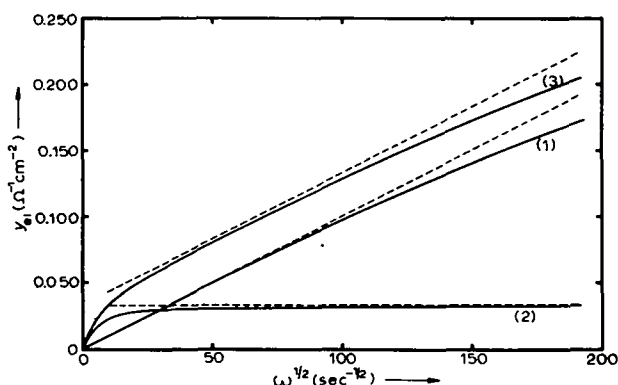


Fig. 3. Plots of  $Y'_{el}$  vs.  $\omega^{\frac{1}{2}}$ : (1)  $p'_1 = 3 \times 10^{-3}$ ,  $\theta_1 = 1.5 \Omega \text{ cm}^2$ ,  $\sigma_1 = 500 \Omega \text{ cm}^2 \text{ s}^{-\frac{1}{2}}$ ; (2)  $p'_2 = 3 \times 10^{-1}$ ,  $\theta_2 = 30 \Omega \text{ cm}^2$ ,  $\sigma_2 = 100 \Omega \text{ cm}^2 \text{ s}^{-\frac{1}{2}}$ ; (3) sum of (1) and (2). The broken lines show the divergence from straight lines.

(ii) The sum-admittance is composed of the admittances of a reversible and a quasi-reversible electrode reaction (*e.g.* this is the case in the example discussed above (Fig. 3) in the frequency range between  $\omega^{\frac{1}{2}} \approx 0$  and  $\omega^{\frac{1}{2}} = 30 \text{ s}^{-\frac{1}{2}}$ ). By substitution of  $p'_1 = 0$  (reversible case) into eqn. (5a) one obtains:

$$\frac{Y'_{el}}{\omega^{\frac{1}{2}}} = \frac{1}{2\sigma_1} + \frac{1}{\sigma_2} \frac{p'_2 \omega^{\frac{1}{2}} + 1}{(p'_2 \omega^{\frac{1}{2}} + 1)^2 + 1} \quad (10)$$

It appears from eqn. (10) that it is possible to evaluate the unknown parameters,  $\sigma_1$ ,  $\theta_1$  and  $\sigma_2$ , by means of a variation method. The accuracy of the results will be largely dependent on the accuracy of the  $Y'_{el}$  values and of the width of the frequency range used. The value of  $C_d$  can be calculated by insertion of the results into eqn. (5b).

(iii) The sum-admittance is composed of the admittances of a quasi-reversible and an irreversible electrode reaction (*e.g.* this is the case in the example discussed above (Fig. 3) at  $\omega^{\frac{1}{2}} > 100$ ). By substitution of  $p'_2 = \infty$  (irreversible case) into eqn. (5a) one obtains:

$$Y'_{el} = \frac{\omega^{\frac{1}{2}}}{\sigma_1} \frac{p'_1 \omega^{\frac{1}{2}} + 1}{(p'_1 \omega^{\frac{1}{2}} + 1)^2 + 1} + \frac{1}{\theta_2} \quad (11)$$

Also, in this case it is possible to evaluate the unknown parameters by means of a variation method. The accuracy is of the same order as discussed above (case ii). The value of  $C_d$  can be calculated by insertion of the results into eqn. (5b).

*Application to the mercury electrode in concentrated HI*

As an example we give the results of an analysis of the impedance of the DME in 57% HI. Experimental details will be described in a subsequent paper.

Figure 4 shows the d.c. current–voltage curve of the cell.

As mercury dissolves in very concentrated hydriodic acid with the evolution of hydrogen gas<sup>9</sup> it is likely that the current–voltage curve of Fig. 4 is composed of the current–voltage curves of two simultaneously proceeding electrode reactions, viz.



The measured current–voltage curve is a so-called mixed current curve and is equal to the algebraic sum of the current–voltage curve for each process<sup>5</sup>.

The impedance of the cell was measured as a function of potential (at 10 potentials in the potential range  $-530$  to  $-630$  mV) and as a function of frequency (420–2000 Hz). The potential region of the impedance measurements is indicated by two arrows in Fig. 4. The ohmic resistance  $R_\Omega$  of the cell was found by measurements of  $Z'$  at some higher frequencies (up to 10 kHz) and extrapolation of  $Z'$  to infinite frequency. The value of  $Y'_{ei}$  was calculated (eqn. (4a)) and plotted against  $\omega^{\frac{1}{2}}$  for each potential. Straight lines were obtained at all potentials: between  $-530$  and  $-590$  mV,  $Y'_{ei}$  increases linearly with  $\omega^{\frac{1}{2}}$ , and at potentials more negative than  $-590$  mV,  $Y'_{ei}$  is independent of  $\omega^{\frac{1}{2}}$ .

Measurements on the  $\text{Hg}/\text{Hg}_2^{2+}$  electrode reaction (e.g. in  $\text{HClO}_4$  solutions)<sup>10</sup>

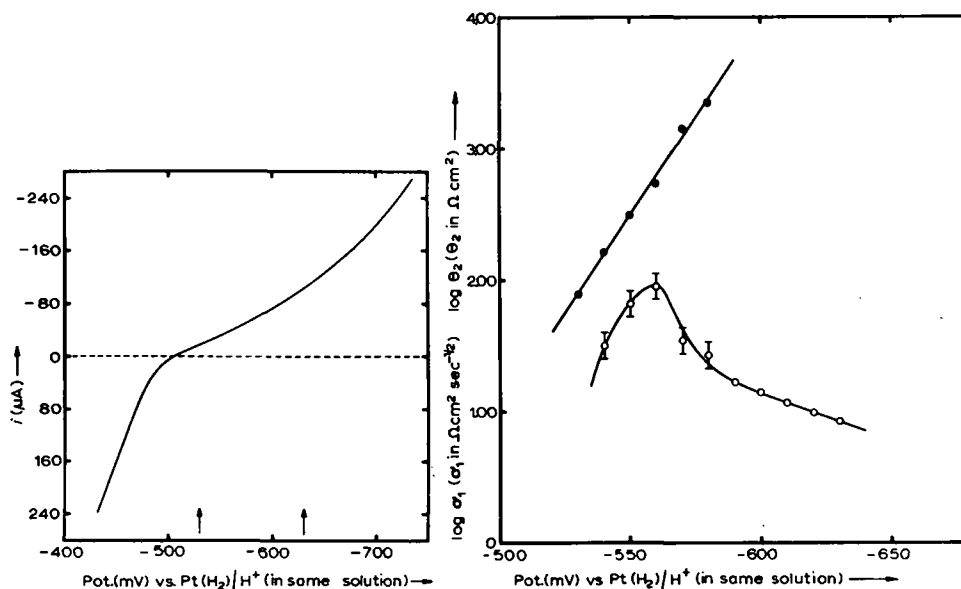


Fig. 4. D.c. current–voltage curve of the DME in 57% HI at 15°C. The vertical arrows indicate the potential region of the impedance measurements.

Fig. 5. Plot of the logarithmic value of the Warburg coefficient  $\sigma_1$  (●) and the activation polarization resistance  $\theta_2$  (○) as a function of potential for the mercury electrode in 57% HI at 15°C.

and in HCl solutions<sup>11</sup>) have always shown that the reaction is reversible. It is therefore reasonable to assume that reaction (I) is reversible. The  $H^+/H_2(Hg)$  electrode reaction (reaction (II)) is known to be irreversible (see *e.g.* Vetter<sup>12</sup>).

Making allowance for the above, the experimental results have been analysed with eqn. (9a). The value of  $\sigma_1$  (reaction (I)) was calculated from the slope of the  $Y_{e1}$  vs.  $\omega^{\frac{1}{2}}$  plot and the value of  $\theta_2$  (reaction (II)) was calculated from the intercept. The results are presented in Fig. 5 in which  $\log \sigma_1$  and  $\log \theta_2$  are plotted against the potential,  $E$ .

The  $\log \sigma_1$  vs.  $E$  plot is a straight line which is in accord with theory<sup>4</sup>. The slope of the line  $-29.45 V^{-1}$  agrees reasonably well with the theoretical slope, corresponding to  $n=2$ .

It is not possible to calculate the value of the diffusion coefficient  $D_{Hg^{2+}}$ , since the formal potential is unknown.

It can be seen in Fig. 5 that the  $\log \theta_2$  vs.  $E$  curve is linear in the potential region  $-590$  to  $-630$  mV which is in agreement with theory<sup>4</sup> and previous measurements on the  $H^+/H_2(Hg)$  electrode reaction<sup>3</sup>. The equation of the line was calculated:  $\log \theta_2 = 5.40 + 7.10 \eta$  (for the  $H^+/H_2(Hg)$  electrode reaction the potential  $E$  is equal to the overpotential  $\eta$ ). The value of the cathodic transfer coefficient  $\beta$  was calculated from the slope of the line, and the value of the exchange current density,  $i_0$ , was obtained from the intercept:  $\beta = 0.40^5$  and  $\log i_0 = -6.6^2$ .

The shape of the  $\log \theta_2$  vs.  $E$  plot in the potential region  $-540$  to  $-590$  mV is of interest (note that this is the potential range in which reaction (I) proceeds measurably): going from cathodic to anodic potentials the value of  $\log \theta_2$  increases more steeply than the linear part at  $E < -590$  mV. When a straight line is fitted through this part of the curve, a value  $\beta = 1.3 \pm 0.3$  is calculated for the transfer coefficient. From a recent study by Krishtalik<sup>13</sup> concerning the hydrogen overpotential on mercury in acidified KI solutions, it is known that  $\beta = 1$  in the case of a barrierless

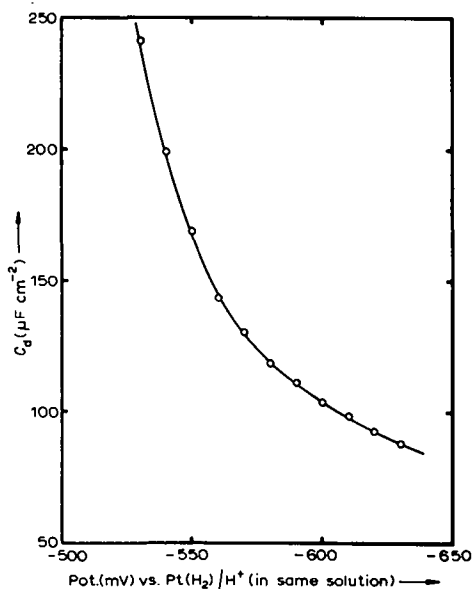


Fig. 6. Capacity-potential curve for mercury in 57% HI at 15°C.

discharge. Since also the shape of the  $\log \theta_2$  vs.  $E$  plot between  $-560$  and  $-630$  mV is qualitatively similar to the plots that can be calculated from the experiments of Krishtalik, it is likely that in the potential region  $-560$  to  $-590$  mV barrierless discharge occurs.

It is not clear, however, why  $\log \theta_2$  decreases at potentials larger than  $-560$  mV. The values of  $C_d$  for the potential region between  $-530$  and  $-590$  mV were calculated from eqn. (9b), while for the potential region  $-590$  to  $-630$  mV eqn. (8) was used for the calculation. The results are presented in Fig. 6. No frequency-dependence of the calculated  $C_d$ -values was found which means that the equivalent circuit of the electrode impedance used for the determination of  $\sigma_1$ ,  $\theta_2$  and  $C_d$  is able to describe the experiments.

#### CONCLUSION

In general, the complex plane method of analysing impedance data can also be applied to cases of two simultaneously proceeding electrode reactions. However, the accuracy of the results depends strongly on the values of the irreversibility quotients of both reactions and on the frequency range in which the measurements are performed.

#### ACKNOWLEDGEMENT

This investigation was supported in part by the Netherlands Foundation for Chemical Research (SON) with financial aid from the Netherlands Organization for the Advancement of Pure Research (Z.W.O.).

#### SUMMARY

The applicability of the complex plane method for the evaluation of the impedance parameters in the case of two simultaneously proceeding electrode reactions is discussed. It is shown that the possibility of the evaluation depends strongly on the values of the irreversibility quotients of both reactions and on the frequency range in which the measurements are performed. The theory is applied to impedance measurements with the dropping mercury electrode in azeotropic HI, in which case a mixed current appears.

#### REFERENCES

- 1 J. E. B. RANDLES, *Discussions Faraday Soc.*, 1 (1947) 11.
- 2 M. SLUYTERS-REHBACH, D. J. KOOIJMAN AND J. H. SLUYTERS, in G. J. HILLS (Ed.), *Polarography* (1964), MacMillan, London, p. 135.
- 3 B. G. DEKKER, M. SLUYTERS-REHBACH AND J. H. SLUYTERS, *J. Electroanal. Chem.*, 21 (1969) 137.
- 4 B. TIMMER, M. SLUYTERS-REHBACH AND J. H. SLUYTERS, *J. Electroanal. Chem.*, 14 (1967) 169.
- 5 C. WAGNER AND W. TRAUD, *Z. Elektrochem.*, 44 (1938) 391.
- 6 M. SLUYTERS-REHBACH, B. TIMMER AND J. H. SLUYTERS, *J. Electroanal. Chem.*, 15 (1967) 151.
- 7 M. SLUYTERS-REHBACH AND J. H. SLUYTERS, *Rec. Trav. Chim.*, 83 (1964) 217, 581.
- 8 M. SLUYTERS-REHBACH AND J. H. SLUYTERS, *Electrochim. Acta*, 11 (1966) 73.
- 9 P. PASCAL, *Nouveau Traité de Chimie Minérale, Tome 5 (zinc-cadmium-mercure)*, Masson, Paris, 1962, p. 586.
- 10 M. SLUYTERS-REHBACH AND J. H. SLUYTERS, *Rec. Trav. Chim.*, 83 (1964) 967.
- 11 R. D. ARMSTRONG, M. FLEISCHMANN AND R. M. THIRSK, *Trans. Faraday Soc.*, 61 (1965) 2238.
- 12 K. J. VETTER, *Elektrochemische Kinetik*, Springer-Verlag, Berlin, 1961, pp. 410-497.
- 13 L. I. KRISHTALIK, *Electrochim. Acta*, 13 (1968) 1045.